Electrical conductivity of ZnS crystals: ZnS crystals as quasi-one-dimensional conductors

Y. Brada
Racah Institute of Physics, The Hebrew University of Jerusalem, Jerusalem 91904, Israel
(Received 30 August 1988)

Due to their special morphology many vapor-grown ZnS crystals behave as quasi-one-dimensional conductors. These faulted single crystals display a highly anisotropic dc conductivity, the conductivity at 90° to the c axis being in some cases up to 10^7 times larger than its counterpart along the c axis. In the latter direction there exist intrinsic builtin electrical fields of different polarities and field strengths. These internal fields are due to charged dislocation layers appearing between different structures and polytypes which have different basal-plane densities. The influence of these phenomena on the ac conductivity has been investigated for frequencies between 5 kHz and 150 MHz which was found to be both direction and frequency dependent. The peculiar properties of these crystals made it possible to distinguish between effects of the electrodes, surface conductivity, dislocations, and bulk conductivity proper. Even at microwave frequencies up to 3 GHz there is a small anisotropy in the electrical conductivity. A theoretical approach developed for the excitation dynamics in random one-dimensional systems which was previously applied to a random barrier model in the case of the anomalous low-frequency behavior of the ionic conductivity in a quasi-one-dimensional superionic conductor, has been found to be appropriate for a quantitative evaluation of the described experiments.

I. INTRODUCTION

A. Structural properties of the crystals

ZnS single crystals grown from vapor at 1100 °C have initially a $2H$ hexagonal structure, but on cooling they undergo structural changes, as the $3C$ cubic structure is the stable configuration at lower temperature.[1] A periodic slip along the screw dislocation along the (000.1) direction is involved, but because of other dislocations and impurity-induced disorder this transformation will generally result in a mixture of structures in these crystals, involving $2H$, $3C$, and polytypic regions,[2] as well as one-dimensional stacking disorder. The (000.1) axis and the ⟨111⟩ cubic axis are codirectional and both have a polar character. The various narrower or wider homogeneous regions are all perpendicular to them, each region of different structure having a slightly different unit-cell dimension within its basal layers. Accordingly, misfits appear in the boundary regions, the tetrahedral bonds being severed at the single bond in the axial direction, so that uncompensated charged layers appear on the boundaries. The existence of these charged boundary layers was deduced from a number of experiments.[3–6]

B. Electronic properties

The crystals used in these experiments and showing direction-dependent conductivity were grown either in a H_2S atmosphere and then had only a weak luminescence, anomalously high photovoltages, and a p-type dark conductance.[7] If, alternatively, the crystals were grown in an Ar-HCl atmosphere they would be strongly luminescent, would have no anomalous photovoltages, and would be n type in the dark.[7] The electron mobility as cited in the literature[8,9] is reported to be in the range of 100–300 $cm^2\,sec^{-1}\,V^{-1}$. In the vicinity of 300 K its temperature dependence is polaronic; i.e., it decreases with the increase of temperature. The presence of strong Al doping induces further ionic scattering,[9] which causes a further decrease in the mobility. The maximum mobility was reported[9] to be somewhat below room temperature, with the mobility decreasing at lower temperature due to the scattering by ionic impurities. At room temperature, the "free" carriers in the bands are due to doping by impurities. Their activation energies are about 5×10^{-2} eV.[10] As both electrons and holes have to be present in order to obtain a persistent photovoltaic short-circuit current,[11] and such an effect exists only in the H_2S grown crystals, it follows that both holes and electrons (in considerable concentrations) are mobile in such crystals, while in the Ar-HCl-grown crystals there seem to be only mobile electrons, since no anomalous photovoltages or short-circuit photocurrents were observed[12,13] in them. The large anisotropy in the dc resistance of the crystals as measured in a direction parallel or perpendicular to the c axis has been observed in various samples and reported by us previously.[12] A classification of the vapor-grown samples has also been made according to their structural composition,[12] which is the dominant factor in their electrical and photovoltaic behavior.

Up to the present work no measurements of ac conductivity were reported in the literature. The existence of the charged boundary layers,[3–8] together with a sufficient concentration of conductance-band carriers in the dark,[10] makes these types of measurements both possible and intriguing.

C. Optical properties and photoconductivity

The absorption edges of all the ZnS configurations lie between 3.744 and 3.639 eV.[14] They are strongly temper-

ature dependent through an internal Franz-Keldysh effect, due to phonon-generated electric fields.[15] Urbach absorption tails are also created, due both to these fields and to the local fields generated by impurities.[15,16] Both photovoltages and photoconductance appear on illumination of the crystal, with photon energies corresponding not only to the band-gap region but even with lower energies, i.e., in the Urbach tail absorption region.[17]

II. EXPERIMENTAL

A. Choice and preparation of the samples

Many crystals were used in this work, all of which were grown by the Crystal Growth Laboratory of the Racah Physics Institute by the techniques described[1] before. Most of the samples were thin platelets (15–500 μm), with the c axis in the plane of the platelet, their widths ranging from 2 to 10 mm. Some needles (2–4 mm thick) of hexagonal cross sections having the c axis along the needle axis were also used. Some samples were used as grown, but others were additionally doped (a) by heating in an electroluminescent ZnS(Al,Cu) powder in a vacuum furnace at 700 °C for two hours, (b) by heating them in In vapor under the above circumstances, and (c) by brushing a temporary In-amalgame coating on the whole surface which was then cleaned off a week later by brushing it with a soft brush while it was immersed in carbon tetrachloride. The first measurements were carried out at room temperature with the samples mounted with Duco cement to a microscope carrier glass. Either silver-paint or In-amalgame electrodes were applied. In all cases the electrodes were applied as parallel bands of several millimeters width on the surfaces of the platelet-like samples. The surface of the platelets is always parallel to the prismatic planes; the only difference between both field directions, parallel or perpendicular to the c axis, lies in their relative directions in the gap between the parallel stripes of the electrodes. This way the contacts were of the same character throughout, in contact with the same type of surfaces. In order to obtain measurable values of currents, specially large samples had to be chosen in all cases. Small thin samples had very low conductivities of the order of 10^{-13}–10^{-10} Si when measured with a dc voltage. It should again be pointed out that there is a great variability between the samples' resistances, even if they were grown in the same batch. This depends not only on the site of growth in the fused-silica tube, but also on the number of height of the barriers. The latter is a function of the difference in the percentage of hexagonality between the neighboring polytypes or structures appearing in the crystal. (The $2H$ structure has a 100% hexagonality, $4H$ crystals have a 50% hexagonality, and the $3C$ structure has a 0% hexagonality.) The larger the difference in hexagonality, the more uncompensated charges will appear in the charge sheets constituting the barriers. For most of the experiments, crystals with low hexagonalities (low birefringences) were chosen so as to obtain more reliable measurements due to their consistently higher conductivities in both dc and high-frequency (HF) measurements. These samples are also more easily influenced by photogenerated charges, as the original charge density on the dislocations is low and so can be quite easily screened by the additional mobile charges. In such crystals the asymmetry of the dc conductance is also markedly decreased. The first group of numbers in the crystal name indicates the particular batch, the next numbers with the prefix HF describe the particular samples used in the high-frequency measurements. The dc measurements carried out during this research showed that the conductances depend not only on the bulk properties and the dislocation-induced barriers but also on the contacts as well, as will be presented in Sec. III. The field direction was either along the c axis ($\mathbf{i} \| \mathbf{c}$) or perpendicular to this axis ($\mathbf{i} \perp \mathbf{c}$). Unless photoexcited on purpose, the samples were covered by black polyethylene covers. The temperature dependence was measured subsequently with a specially adapted "Helitran" cryostat. At lower temperature, in undoped samples the conductivity diminished rapidly, but in doped samples, impurity-band conduction could be observed. Details will be reported in a later publication.

B. The measuring instruments

The conductance-measuring systems were built around two instruments: (a) a Model 75C ac bridge (Boonton Electronics) for the range of 5–500 KHz and (b) a Model TF 1245 Circuit Magnification Meter (Marconi Instruments), which was used for the range of 0.3–150 MHz. The voltages used were in the vicinity of 2–4 V rms.

C. The influence of the contacts

There exists no known practical way of affixing Ohmic contacts to insulating ZnS crystals without drastically changing the crystal properties. Such techniques as applying molten In do introduce unwanted changes. Ohmic behavior was observed only in the case of strongly surface-doped samples, as in cases (a) and (b) of the preceding section. Normally both the silver-paint and the In-amalgame electrodes have a blocking character, which is most noticeable in the measurements carried out with the field perpendicular to the c axis direction ($\mathbf{i} \perp \mathbf{c}$). Figure 1 describes the result of such an experiment. In this case the ac measurements prove that the carriers (because of the low mobility of the holes, most of the current in the sample will be due to electrons) are largely inhibited from passing through the electrode-crystal barrier. The system can be described as a slab of material with low conductance between two almost blocking electrodes. In the first approximation the behavior of such a system is similar to a serial RC circuit, the relaxation time (t) of which depends on the following material constants:

$$t = \epsilon_0 / n \mu_0 e \text{ sec} , \tag{2.1}$$

where μ_0 is the mobility, n is the carrier concentration, ϵ_0 is the static dielectric constant, and e is the magnitude of the charge of the electron. The relaxation time is typically in the MHz range, so that the in-phase current will saturate at high frequencies, as can be seen in Fig. 1. It is, however, to be pointed out that in this case the current is due to the internal equilibrium charge of the crystal,

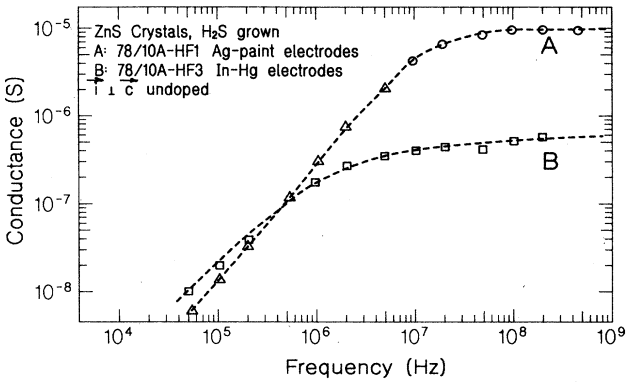

FIG. 1. Conductance measurements on two ZnS crystals in a perpendicular direction to the c axis, no internal barriers are involved. Crystal 78/10A-HF1 (H_2S), three platelets connected at the corner (30° angles); only one platelet has electrical connections. Average thickness of measured part, 114 μm; width, 10.0 mm. Average distance between silver paint strips is 1.0 mm. Crystal 78/10A-HF3 (H_2S), single platelet; thickness, 245 μm; width, 5.67 mm. Distance between In-Hg electrodes, 1.86 mm.

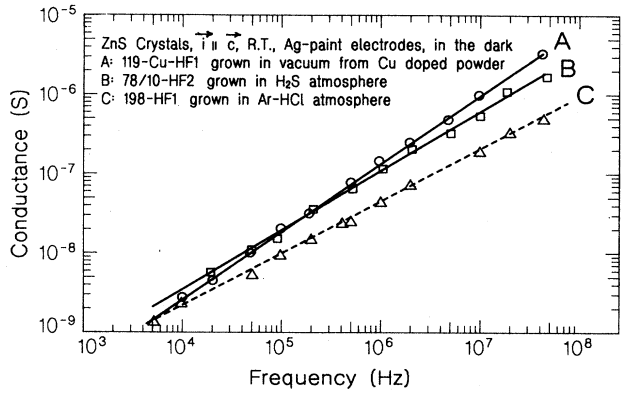

FIG. 2. Conductance in ZnS crystals with the field applied parallel to the c axis. *A*, Vacuum grown from Cu-doped ZnS powder; *B*, grown in H_2S atmosphere; *C*, grown in Ar-HCl atmosphere. All measured in dark at room temperature with Ag-paint electrodes. Crystal 119-Cu-HF1, unevenly surfaced platelet. Average thickness, 530 μm; width, 10.0 mm. Distance between Ag-paint electrodes, 1.7 mm. Crystal 78/10-HF2 (H_2S), single platelet. Thickness, 126 μm; width, 8.9 mm. Distance between Ag-paint electrodes, 0.78 mm. Crystal 198-HF1, single hollow needle, flattened hexagonal cross section. Thickness of walls about 150 μm; width, 1.24 mm. Distance between Ag-paint electrodes, 2.0 mm.

which is transported forth and back between the high-resistance contacts in phase with the applied external voltage. Therefore $i \propto \Sigma Q$, where ΣQ is the total charge moved from one contact area to the opposite contact area in accordance with the oscillations of the electrical field. If the total "free" floating charge is Ne, then as long as $(\mu_0 V/\nu L) > L$ (where ν is the frequency, V the external voltage, and L the distance between the electrodes), ΣQ in unit time will be proportional to νNe, i.e., also proportional to the number of times the internal equilibrium charge is transported from one contact barrier to the second contact. If this would have been an ordinary series RC circuit, the conductance would depend on the square of the applied frequency, and would not have a linear dependence.

D. The influence of internal barriers

A completely different result is obtained when the measurements are carried out with the field direction along the c axis, as in Fig. 2. The resulting conductance is sublinear in frequency and there is no saturation even at the highest frequencies. The movement of the carriers is in this case inhibited by a great number of potential barriers. Each of the charged dislocation regions becomes a barrier to the carriers having the identical sign of charge. In this case the influence of the electrode barriers will be insignificant. On the other hand, by creating many free carriers, for example, by light, the internal charge of the barriers can be largely canceled by space charges (both free and bound) of opposite signs. Such an experiment is represented by Fig. 3, which shows the gradually changing character of the ac conduction from a power-law dependence of the conductivity on the frequency with a power of 0.64 (I) to a stage when practically all the internal barriers are compensated for by both the floating and the fixed space charges (III). The fixed space charges may be due to the donors, acceptors, or traps in various charge states. With the highest illumination, one obtains a very similar current-frequency characteristic, as in the internal-barrier-free case in Fig. 1. It should be noted that we reported a negative differential photovoltage in some ZnS crystals.[17] This effect occurs with a strong uv monochromatic illumination, which results in an open-circuit anomalous photovoltage: the voltage actually decreases with an increase in intensity of the exciting light[17] above a certain threshold. The negative differential photovoltage is an additional indication that the internal intrinsic fields diminish because of the light-generated

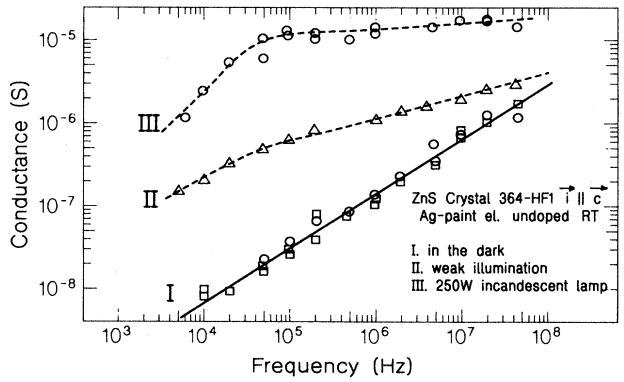

FIG. 3. The changes in the conductance when a crystal is being illuminated. I is the conductance in the dark, II the total conductance on weak illumination, III the same with 250-W incandescent-lamp illumination. Crystal 346-HF1 (A-HCl), single platelet, uneven surface but smooth. Average thickness, 350 μm; width, 4.2 mm. Distance between Ag-paint electrodes, 0.71 mm.

TABLE I. Summary of a number of experiments on different crystal. f^0 region means that there exists a region in which the conductance is frequency independent. HF exp. means the value of the exponent of the frequency dependence of the conductance at the highest frequencies used. The first group of numbers identifies the growth batch, while the second number, after HF, identifies the individual sample.

Crystal	Gas	Contact	f^0 region	HF exp.	Remarks
78/10A-HF1	H_2S	Ag-pnt	yes	0.0	field perp. to c axis no doping
78/10A-HF3	H_2S	In-Hg	yes	0.0	no illumination
		Field along c axis in all the following samples			
78/10A-HF2	H_2S	Ag-pnt	no	0.89	no doping
173-HF1	Ar-HCl	Ag-pnt	no	0.83	no illumination
198-HF1	Ar-HCl	Ag-pnt	no	0.66	
78/11-HF4	H_2S	Ag-pnt	yes	0.80	doped Al-Cu
78/11-HF1	H_2S	In-Hg	yes	0.74	doped In-Hg
78/11-HF7	H_2S	Ag-pnt	yes	0.46	doped In-vapor
	H_2S	Ag-pnt	no	0.80	after 100 days
		Influence of light			
79/10-HF2	H_2S	Ag-pnt	no	0.78	no light, no doping
	H_2S	Ag-pnt	no	0.76	weak incand. light
	H_2S	Ag-pnt	yes	0.00	250 W incand. lamp
346-HF1	Ar-HCl	Ag-pnt	no	0.64	no light, no doping
	Ar-HCl	Ag-pnt	no	0.27	uv light
	Ar-HCl	Ag-pnt	almost	0.07	strong uv light
78/11-HF1	H_2S	In-Hg	yes	0.74	doped, no light
	H_2S	In-Hg	yes	0.16	doped, uv light

charges inducing screening effects. Table I sums up some of the results obtained on a number of samples at room temperature, either in the dark or illuminated in the uv by a discharge lamp (Hg, 500 W) or an incandescent lamp (Quartz-Iodine, 250 W), the light of which was in both cases directed on the crystal with the help of fused-silica optics. These latter measurements also gave results similar to Fig. 3.

E. Surface effects

In order to check for any possible surface effects in the measured conductivity-frequency characteristics, as shown previously, we deliberately doped a number of samples on the surface. Several methods were used. In the first case the crystals were placed in an electroluminescent ZnS powder containing Al and Cu impurities inside a Pyrex tube. This tube was evacuated and then heated to 700 °C for the period of two hours. The second method used was placing the samples in In vapor under the same circumstances, while in the third experiment the samples were temporarily coated with the same In amalgame as was used for some of the contacts. All these processes introduced an appreciable surface conductance. This was due to a thin conducting layer bridging the barriers on the surface. Figure 4 shows the conductance of a crystal after the powder treatment. The results prove that the conductivity is a sum of two processes: the frequency-independent surface conduction through a thin conducting layer, and the frequency-dependent conduction of the bulk of the crystal. This constitutes a parallel connection of two media with different characteristics of conduction. In addition, the heating introduced lasting changes in the conductance. Figures 5(a) and 5(b) show the measurements on In-doped crystals. With the crystals fresh from their indium vapor treatment, we could observe under the microscope lines of very small drops of the In metal on the surface of the crystals. These condensations occurred preferably on the lines dividing the different crystalline structures, just as when very fine TiO_2 powder was sprinkled on such samples,[18] which is probably due in both cases to attracting electric fields reaching the surface of the samples. While the crystal behavior shown in Fig. 5(a) was of a sample with a low concentration of In on the surface, Fig. 5(b) shows the behav-

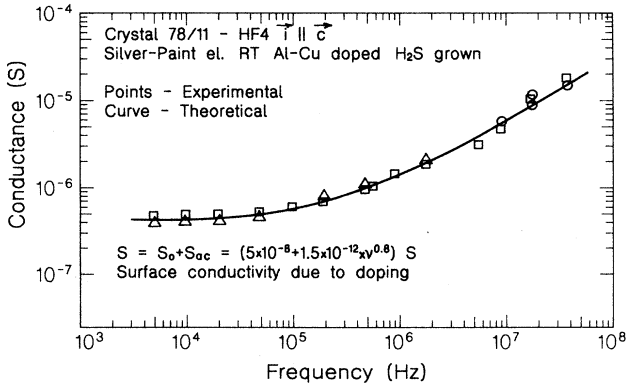

FIG. 4. The conductance along the c axis in a surface-doped crystal (Al-Cu doping). Crystal 78/11-HF4 (H_2S), single platelet, heated in Al-Cu electroluminescent ZnS powder. Thickness, 120 μm; width, 3.5 mm. Distance between Ag-paint electrodes, 1.1 mm.

ior of a similar, but heavily doped sample. A slow decrease of the low-frequency conductance as represented by the various lines in Figs. 5(a) and 5(b) with time occurs in both cases: about 21 days passed between each measurement. These changes are probably due to a combination of diffusion and surface oxidation. In all these cases the influence of the surface conductivity is of course most strongly visible at the lower frequencies; as a result of the fast increase of the bulk conductance with frequency in the undoped crystals, the high-frequency current will be carried by the bulk of the crystal, overshadowing the surface conductance of the thin surface layers at the high frequencies. As can be seen from the experimental data in Figs. 5(a) and 5(b), no lasting effects occurred due to surface doping, so that the influence of permanent

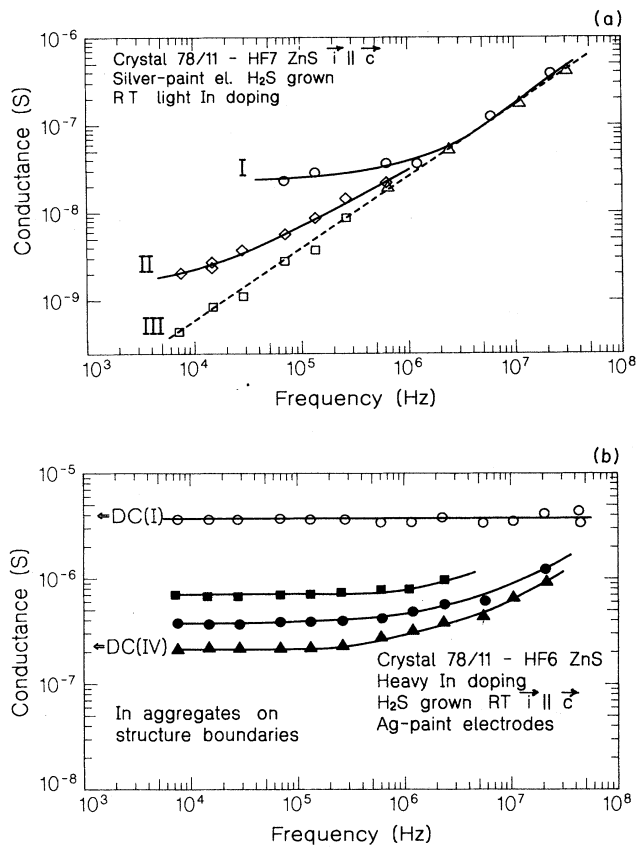

FIG. 5. The frequency dependence in In-vapor-treated crystals. (a) is of a lightly doped sample; about 21 days passed between measurements I, II, and III. (b) shows the conductance of heavily In-doped crystals. About 21 days passed between measurements I, II, III, and IV. Aggregates of In were visible on the surface along the boundary lines between different structures immediately after the surface treatment. (a) Crystal 78/11-HF7 (H_2S), single platelet, In-vapor doped, rough surface. Thickness, 103 μm; width, 4.10 mm. Distance between Ag-paint electrodes, 0.50 mm. (b) Crystal 78/11-HF6 (H_2S), double platelet, 120° angle between the platelets, connecting seam along c-axis direction, low hexagonality, rough surface, heavy In doping. Thickness, 122 μm; total width, 4.34 mm. Distance between Ag-paint electrodes, 1.30 mm.

structural damage as the reason for the observed changes can be ruled out. Also, no annealing of defects was previously observed at room temperature; on the contrary, purely hexagonal samples showed thin layers of more cubic character, which are thermodynamically more stable below 1060 °C. On the other hand, it should be pointed out that the existence of a doped surface layer reduced or even abolished the blocking character of the various electrodes, so that the dc and low-frequency conductances were of the same values.

F. The anisotropy of the conductivity as a function of frequency

Extrapolating Fig. 3, we would expect the disappearance of the conduction anisotropy at frequencies between 10^9 and 10^{10} Hz. In order to check this assumption we carried out measurements at microwave frequencies. Square platelets of faulted ZnS crystals were introduced on a special Teflon pin in the electrical field maxima of the resonant cavities, and the resulting change in the measured values of the Q of the cavity was recorded for two cases: when the square platelets were rotated so as to have the electrical field vector in one case along, and in the second measurement perpendicular to, the direction of the c axis, with the direction of the vector in both cases lying parallel to the large plane of the platelet. These measurements were made at two frequencies: 8×10^9 and 3.5×10^{10} Hz. At the lower frequency in some samples there was still a very small change in the conductivity on their rotation, the factor being 3–4 times, while with the same samples no measurable change was seen when the higher frequency was employed. At these frequencies the influence of the barriers is minimal, as at the very high frequency the *Schubweg* will be less than 0.1 μm and only in regions of this size and smaller will the barriers still tend to interact with the movement of the carriers. On the other hand, in very densely faulted crystals the internal fields are very low, as is apparent from the very low external photovoltages.[19,17] In other words, the barriers are very low, and practically "transparent" to the carriers.

III. DISCUSSION AND CONCLUSIONS

A. The character of the conduction

Table I and Figs. 1–6 indicate the following features of electrical conductance in faulted single crystals of ZnS. There is a basic difference between the conductance parallel to the c axis and that perpendicular to this direction. As both the materials of the crystal and their electrodes are the same in both cases, the difference can only be due to the structural properties of these crystals, which are direction dependent in the same way. In the first case, along the c axis, a functional dependence of the following form is observed:

$$G = G_0 f^a + G_{dc} \,. \tag{3.1}$$

Here G is the conductance, G_0 is a proportionality coefficient, f is the frequency, a is a sample-dependent ex-

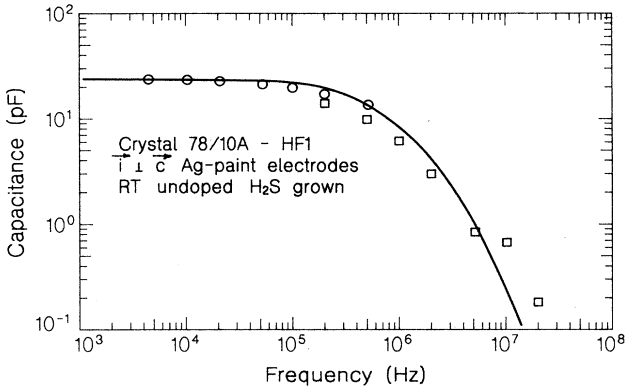

FIG. 6. The capacitance of a crystal measured in the perpendicular direction to the c axis. Crystal 78/10A-HF1 (H_2S), triplet platelet connected on the corner, 30° angles, only one platelet has electrical connections, seam along c-axis direction. Average thickness of measured part, 114 μm; width, 10.0 mm. Average distance between Ag-paint electrodes, 1.0 mm.

ponent which is always smaller than 1, and G_{dc} is the dc conductance. In the second case we obtain at low frequencies a frequency dependence of the form

$$G = G_0 f^b , \tag{3.2}$$

with $b \approx 1$ tending to zero at MHz frequencies. In the direction of the common c axis the conduction is very similar to that of a one-dimensional conductor: the different homogeneous structures themselves are internally much more conducting as compared to the conductance across the boundary layers between these homogeneous structures, so that it is possible to use theories which were developed for the one-dimensional case.[20,21] The electrical conduction in such structures can be considered as a special case of excitation in a random one-dimensional system.[21] Such methods were previously applied to quasi-one-dimensional conduction in a superionic conductor, namely Hollandite.[20] In that case, the carriers are potassium ions which are blocked from continuing along a one-directional structure by structural gaps which in Hollandite are the energy barriers to be overcome. These gaps play the same role as the charged boundary layers in our crystals. The theory will also be applied to our results. For a quantitative evaluation, values of some parameters have to be set in the first place. We will use the symbols of the original paper.[20] The concentration of free carriers in our samples varies at room temperature between 10^{11} and 10^{14} cm^{-3}. The mobility of the electrons is between 200 and 300 cm^2 sec^{-1}V^{-1}. The height of the barrier will be evaluated later from the internal electrical fields created by the charged dislocation sheets[3] and also by considering the value of the dc current. Using the Einstein relation,

$$\mu_0 = eD/k_B T , \tag{3.3}$$

where μ_0 is the mobility, e is the electronic charge, k_B is the Boltzmann constant, D is the diffusion constant, and T is the temperature. From this relationship the value of D is 5.18 cm^2 sec^{-1} when the mobility was taken to be 200 cm^2 sec^{-1} V^{-1}. Using this value find the root mean square of the diffusion length is

$$a_{rms} = \sqrt{2Dt} = 3.22 \text{ cm} , \tag{3.4}$$

with $t = 1$ sec. We will assume with Ref. 20 that the transport across a barrier is thermally activated and compute the penetration probabilities:

$$\Gamma_{n,n+1} = \Gamma_{n+1,n} = f_0 \exp(\Delta_{n,n+1}/k_B T) , \tag{3.5}$$

where $\Gamma_{n,n+1}$ is the penetration probability from sector n to sector $n+1$, f_0 is the frequency of penetration attempts, and $\Delta_{n,n+1}$ is the height of the energy barrier between the sectors. L will be the average distance between barriers, which in our experiments was about 10^{-4} cm. The attempt frequency can be evaluated as

$$f_0 = D/(a_{rms} L) = 1.61 \times 10^4 \text{ sec}^{-1} . \tag{3.6}$$

The energy of the barriers will be between a minimum value, below which they will not influence the carrier transition, and a maximum value, which in our case will be the one of the barrier between a $3C$ and $2H$ structure. Using the method of Ref. 20, we will assume an exponential distribution of barrier heights so that the probability of obtaining a value of Δ between these boundary values is

$$W(\Delta) = W_0 \exp(-\Delta/k_B T) , \tag{3.7}$$

with $\Delta_0 \le \Delta \le \Delta_1$ and $W(\Delta) = 0$ outside this range. The maximum value of Δ_1 is given by the highest fields existing in our samples,[3] i.e., about 1×10^4 V cm^{-1} in the narrow segments of $L = 10^{-4}$ cm. In this case we will obtain a barrier height of about 1 eV. In addition, we find a much more numerous population of segments having very low fields of the order of 10^3 V cm^{-1} and in these cases, with segments of the above dimension, we obtain barriers of about 0.1 eV. By averaging the values of Δ as given by Eq. (3.7) we obtain[20]

$$\Delta_{av} = k_B T_m + \Delta_0 \tag{3.8}$$

and as T_m has been found to be about 700 K in most of our experiments, we obtain a value of Δ_{av} of about 0.16 eV. One can also try to evaluate these parameters from measurements of current. Using the relationship[20]

$$\frac{dq_n}{dt} = I = \sum_{\sigma = \pm 1} \Gamma_{n,n+\sigma} \{ (q_{n+\sigma} - q_n) + [eLE(t)] \times (\sigma q_{n+\sigma})/(k_B T) \} , \tag{3.9}$$

where q_n is the charge in the nth segment and $E(t)$ is the field. In the dc case $E(t) = E_0$, and the difference in carrier concentration in two segments will also be negligible. Because of the weak fields employed (approximately 10 V cm^{-1}) the contribution of the field is very small, at the most it is of the order of several percent of the basic concentration q_n:

$$\delta q = (eLE_0 q_n)/(k_B T) \approx 3.87 \times 10^{-2} q_n . \tag{3.10}$$

It is possible to compute $\Gamma_{n,n+1}$ and from dc measurements at 300 K:

$$I = 10^{-11}\ \text{Å} = \frac{dq_n}{dt} = \Gamma_{n,n+1}(eLE_0 q_n)/(k_B T) \ . \qquad (3.11)$$

With a typical case of a carrier density of 5×10^{12} cm^{-3}, then in a sector 10^{-4} cm long, 0.5 cm wide, and 4×10^{-2} cm thick there will be about 10^7 carriers, which means about 1.6×10^{-12} C of charge. Using Eq. (3.4) one obtains at 300 K a value of $\Gamma_{n,n+1}=162$ and from this $\Delta=0.12$ eV. This is a value similar to the one obtained from the average value of the fields inside the crystal segments. The good agreement is somewhat fortuitous but is nevertheless a result of previously measured values.[3,5] Using this theory[20] we also have to consider its frequency limitation, which, considering the properties of our samples, demands that $f \ll 10^9$ Hz. This limit has indeed not been reached in the ordinary frequency-dependent conductance measurements. In full accordance with the theory, we have shown experimentally that the barriers will lose their effectiveness at microwave frequencies. In Ref. 20 the authors developed a theory for the temperature dependence of the exponent in Eq. (3.1), which fit well the experimental results as measured on Hollandite. The exponent could be written as

$$a = (1 - T/T_m)/(1 + T/T_m) \ , \qquad (3.12)$$

where T is the temperature in K, and T_m describes a mobility transition temperature where the conductance becomes approximately frequency independent. In the nonilluminated samples, as seen in Table I, the value of the exponent a is always smaller than 1 and its magnitude varies between 0.4 and 0.8, which would correspond to T_m values of between 700 and 2700 K corresponding to thermal energies between 0.06 and 0.2 eV. At such temperatures the above-mentioned barriers would certainly not impede the movement of the carriers anymore. Because of the instability of both the structural properties of the crystals and of the electrodes, especially at temperatures above 400 K, it is difficult to observe changes of the slopes, while other, irreversible changes of conductance occur. There were some indications of a lower exponent at higher than room-temperature measurements and a markedly higher exponent was observed at lower temperatures.

B. Capacitance measurements

The value of the measured capacitance is also frequency dependent. With the field applied in the direction perpendicular to the c axis, the full blocking electrode junction capacitance is measured at low frequencies—about 40 pF—in the sample shown in Fig. 6. The conduction relaxation time in our crystals was about 10^{-6}–10^{-7} sec; therefore, at frequencies of 10^6–10^7 sec^{-1} the quantity of accumulated charges diminishes drastically and the measured capacitance decreases further with frequency to its limiting values, due to the sample size and dielectric constant of the material. This also can be seen in Fig. 6. Other insulating inorganic crystals showed the same behavior, as all of these additional samples were homogeneous and had no internal barriers. The measurements of capacitances along the c axis showed very low values even at low frequencies, where changes were between 1 and 0.5 pF at the utmost. This proves again that the internal barriers have an overwhelming influence.

IV. CONCLUSIONS

It has been shown that in faulted, as-grown single crystals of ZnS, a special type of frequency-dependent conductance can be observed. In conductance measurements along the common c axis of all the crystalline structures the crystal behaves as a quasi-one-dimensional conductor with internal potential barriers. These barriers are due to structural changes between the different crystal types because of the variation in basal-plane spacings. These changes introduce charged dislocation boundary layers perpendicular to the common c axis. These charge barriers can be compensated for by photoexcited carriers up to the complete disappearance of their influence due to free-carrier screening effects. The results of the experiments were treated qualitatively with the help of a theory of the excitation dynamics of random one-dimensional systems as applied previously to the electrical ac conduction in quasi-one-dimensional superionic conductors.

Surface-doping effects were also investigated. The conductance of the doped surface layers was observed to constitute a shunt to the internal bulk conductance, providing a very effective bypass for the dc conductance. These very thin layers of doped material are not stable and their influence diminishes with time. In conductance measurements across the c axis, where no internal barriers impede the passage of carriers, the major influence was found to be due to the blocking behavior of the external contacts. Preliminary accounts of these results were given in Refs. 22 and 23.

ACKNOWLEDGMENTS

Thanks are due to Sala Binenboim of the Crystal Growing Laboratory of the Racah Physics Institute for growing the crystals, to Professor S. Alexander for triggering this research, and to Professor I. T. Steinberger for critical reading of the manuscript. Thanks are also due to I. Yatsev for numerous measurements. This work was supported in part by the Israel Commission for Basic Research.

[1] I. T. Steinberger, E. Alexander, Y. Brada, Z. H. Kalman, I. Kiflawi, and S. Mardix, J. Cryst. Growth **13/14**, 281 (1972).
[2] S. Mardix, Z. H. Kalman, and I. T. Steinberger, Acta Crystallogr. A **24**, 464 (1968).
[3] G. Shachar, Y. Brada, E. Alexander, and Y. Yacobi, J. Appl. Phys. **41**, 723 (1970).
[4] B. G. Yacobi and Y. Brada, Phys. Rev. B **10**, 665 (1974).
[5] S. G. Ellis *et al.*, Phys. Rev. **109**, 1800 (1958).
[6] B. G. Yacobi and Y. Brada, J. Appl. Phys. **47**, 1243 (1976).
[7] G. Shachar, Y. Brada, and I. T. Steinberger, J. Appl. Phys. **41**, 4938 (1970).
[8] F. A. Kroger, Physica **22**, 637 (1956).

[9]H. Aven and C. A. Mead, Appl. Phys. Lett. **7**, 8 (1965).
[10]Y. Brada (unpublished).
[11]J. Tauc, *Photo and Thermoelectric Effects in Semiconductors* (Pergamon, New York, 1962).
[12]G. Shachar and Y. Brada, J. Appl. Phys. **41**, 3127 (1970).
[13]G. Shachar, Y. Brada, and I. T. Steinberger, Appl. Phys. **42**, 872 (1971).
[14]O. Brafman and I. T. Steinberger, Phys. Rev. **143**, 501 (1966).
[15]B. G. Yacobi *et al.*, Phys. Rev. B **11**, 2990 (1975).
[16]B. G. Yacobi and Y. Brada, Solid State Commun. **18**, 135 (1976).
[17]G. Shachar and Y. Brada, J. Appl. Phys. **39**, 1701 (1968).
[18]O. Brafman, G. Shachar, and I. T. Steinberger, J. Appl. Phys. **36**, 668 (1965).
[19]G. Shachar, S. Mardix, and I. T. Steinberger, J. Appl. Phys. **39**, 2485 (1968).
[20]J. J. Bernasconi, H. V. Bayeler, S. Strassler, and S. Alexander, Phys. Rev. Lett. **42**, 819 (1979).
[21]S. Alexander, J. Bernasconi, W. R. Schneider, and R. Orbach, Rev. Mod. Phys. **53**, 175 (1981).
[22]Y. Brada, Bull. Isr. Phys. Soc. **25**, 29 (1979).
[23]Y. Brada, Abstracts of the Second International Conference on II-VI Compounds, Aussois, France, 1985 (unpublished).